Towards Analytical Solution for 3D SPECT Reconstruction with Non-Uniform Attenuation and Distance-Dependent Resolution Variation: A Monte Carlo Simulation Study

Hongbing Lu*, Junhai Wen, Xiang Li, Tianfang Li, Guoping Han, and Zhengrong Liang

Dept. of Radiology, State University of New York/Stony Brook

ABSTRACT

Based on Kunyansky's and our previous work, an efficient, analytical solution to the reconstruction problem of myocardial perfusion SPECT has been developed that allows simultaneous compensation for non-uniform attenuation, scatter, and system-dependent resolution variation, as well as suppression of signal-dependent Poisson noise. To avoid reconstructed images being corrupted by the presence of Poisson noise, a Karhunen-Loeve (K-L) domain adaptive Wiener filter is applied first to suppress the noise in the primary- and scatter-window measurements. The scatter contribution to the primary-energy-window measurements is then removed by our scatter estimation method, which is based on the photon detection energy spectrum and a triple-energy-window acquisition protocol. The resolution variation is corrected by a depth-dependent deconvolution, which, being based on our central-ray approximation and a distance-frequency relation, deconvolves the scatter-free data with a measured accurate detector-response kernel in frequency domain. Finally, the deblurred projection data are analytically reconstructed with compensation for non-uniform attenuation by an algorithm based on Novikov's explicit inversion formula. The preliminary Monte Carlo simulation results using a realistic human thoracic phantom demonstrate that, for parallel-beam geometry, the proposed analytical reconstruction scheme is computationally comparable to filtered backprojection and quantitatively equivalent to iterative maximum *a posteriori* expectation-maximization reconstruction. Extension to other geometries is under progress.

Keywords: Analytical reconstruction, non-uniform attenuation, resolution variation, object-specific scatter, signal-dependent Poisson noise, attenuated Radon transform

1. INTRODUCTION

SPECT (single photon emission computed tomography) is a cost-effective, widely-used diagnostic modality which utilizes radiotracers to directly label tissue functions. It is currently the gold standard for chest pain evaluation in emergence room across this nation. Most SPECT protocols for clinical use support only qualitative reconstruction. Quantitative SPECT is in great demand for more accurate diagnostic evaluation and is the goal of much effort in SPECT imaging research, especially in the development of image reconstruction and compensation methods. To achieve this goal, we have to address a number of factors that significantly degrade the acquired projection data. These factors include photon attenuation due to absorption and Compton scatter of primary photons, depth-dependent detector response variation, inclusion of scattered photons in the measurement, and random inconsistencies, such as Poisson noise of radionuclide decay and photon detection.

The variety of existing SPECT algorithms can be classified into a family of iterative techniques [1-5] and a wide class of analytical (non-iterative) methods [6-18]. Iterative reconstruction algorithms have the advantages of modeling the noise nature and realistic mathematical models of the measurements. Therefore, they can correct for all the degradation factors described above. However, their iterative nature demands a heavy computational effort and furthermore their associated cost-function regularization and iterative convergence have been remained as research topics for years. The analytical methods are considerably faster and widely used in clinic. It is also straightforward to analyze the noise property of the reconstructions for clinic assessment. But, given the realistic mathematical models of the SPECT measurements, it's difficult to derive an explicit inversion formula, which is essential for the design of an analytical method. In the past decades, analytical methods that can simultaneously correct for uniform attenuation and distance-dependent resolution

* hblu@clio.rad.sunysb.edu; phone 1 631 444-7921; fax 1 631 444-6450; Dept. of Radiology, State University of New York, Stony Brook, NY, USA 11794-8460.

Medical Imaging 2002: Image Processing, Milan Sonka, J. Michael Fitzpatrick, Editors, Proceedings of SPIE Vol. 4684 (2002) © 2002 SPIE · 1605-7422/02/$15.00

variation (DDRV) have been extensively developed and investigated for reconstruction of three-dimensional (3D) SPECT [6, 9, 10, 13-16, 18]. However, creation of the analytic SPECT reconstruction algorithm operative in the case of arbitrary realistic attenuation coefficients has become possible only recently. Based on the explicit inversion formula for the attenuated Radon transform discovered by Novikov (2000), Kunyansky presented a new reconstruction algorithm, which allows for accurate non-iterative SPECT reconstruction in the presence of arbitrary realistic attenuation. Numerical examples showed that the algorithm is capable of accurate image reconstruction even in the case of non-uniform attenuating media [19, 20]. However, the algorithm only takes the effect of non-uniform attenuation into account. Other image degradation factors, such as resolution blurring and photon scattering, are not included. In this study, based on Kunyansky's and our previous work, we develop an efficient, analytical solution to the reconstruction problem of myocardial perfusion SPECT, which compensates simultaneously for non-uniform attenuation, scatter, and system-dependent resolution variation, as well as suppression of signal-dependent Poisson noise.

2. METHODS

In general, the noise-free sinogram with parallel projections in 3D SPECT with non-uniform attenuation, distance-dependent spatial resolution, and scatter radiation can be expressed as

$$\bar{p}_h(\xi,\phi,z,\mu) = \int d\eta \times [\int_{z',\xi'=-\infty}^{\infty} d\xi' dz' f(\xi',\eta,z') h(\xi-\xi',\eta,z-z') e^{-\int_{\eta}^{\infty}\mu(\xi',\eta',z')d\eta'}] + r(\xi,\phi,z). \quad (1)$$

where $\mu(\xi,\eta,z)$ is the attenuation coefficient map of the body, $h(\xi,\eta,z)$ is the depth-dependent spatial resolution function of a SPECT system at "distance" η, $f(\xi,\eta,z)$ denotes the radiotracer activity distribution inside the body, and $r(\xi,\phi,z)$ means the background events such as scatter contribution.

With the existence of noise, we propose a non-iterative reconstruction scheme that corrects simultaneously for all the above degrading factors, as shown in Figure 1. In following subsections, we will describe our analytical reconstruction scheme in detail.

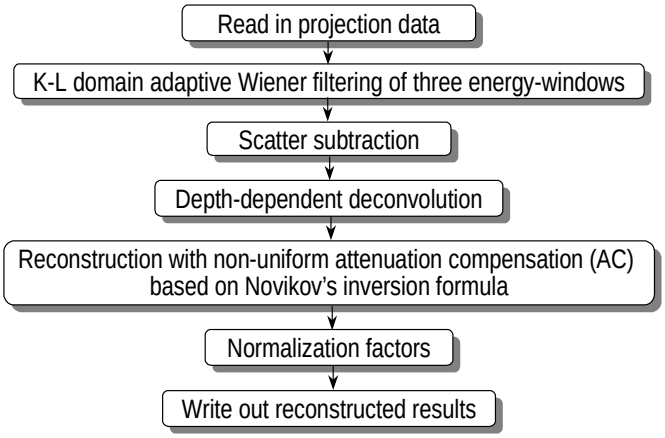

Figure 1. Flow chart for proposed reconstruction scheme.

2.1 K-L Domain Adaptive Wiener Filtering for Accurate Treatment of Poisson Noise

As is true for all inverse solutions, analytical reconstruction methods that compensate for the attenuation-resolution effects can be highly susceptible to data noise and model errors. Therefore, these methods should be regularized adequately so that they are numerically robust and can yield quantitatively accurate images. To avoid reconstructed images being corrupted by the presence of severe noise and conspicuous artifacts, we first apply our K-L domain adaptive Wiener filter, which accurately treats the signal-dependent Poisson noise in the primary and scatter window measurements.

The task of spatial filtering of signal-dependent Poisson noise can be greatly simplified by first applying the Anscombe transform to all the projection data, which converts Poisson distributed noise into Gaussian distributed one with a constant variance [21]. That is, if x is Poisson distributed with mean equal to λ, then $y= (x+3/8)^{1/2}$ can be

approximated as Gaussian distributed with mean equal to $(\lambda+1/8)^{1/2}$ and variance of 0.25. Therefore, by Anscombe transformation, the noise becomes signal independent and can be expressed mathematically as an additive term. In this situation, the noise covariance matrix of the transformed projection data is the identity matrix (with unit variance and being uncorrelated) multiplied by 0.25.

It has been proved that in the K-L domain, the noise property of constant variance remains for all components [22]. By applying K-L transform on Eq.(1), we have

$$\boldsymbol{g} = A_M \boldsymbol{p}_{an} = A_M \boldsymbol{p}' + A_M \boldsymbol{n}' = \boldsymbol{p}_1 + \boldsymbol{n}_1 \tag{2}$$

where $A_M = A \otimes I_M$ and A is a $K \times K$ matrix composed of eigenvectors of the covariance matrix K_t between different sinograms. Notation I_M denotes a $M \times M$ identity matrix and $\otimes$ represents the Kronecker product. By separatebility assumption [22, 23], the Wiener restoration in the K-L domain can be expressed by K independent filters each for one principal component,

$$\hat{p}_{1i} = d_i K_s (d_i K_s + \sigma_n^2 \boldsymbol{I_M})^{-1} \boldsymbol{g_i}, \quad i=1, 2, \ldots, K \tag{3}$$

where K_s is the spatial covariance within the sinograms, d_i is the i-th eigenvalue of the covariance matrix K_t, and σ_n^2 is a constant equal to 0.25. If spatial stationarity for each principal component is utilized, the 2D Wiener filter in the K-L domain is then expressed as

$$H(\omega_s, k_\theta) = \frac{S_{g_i}(\omega_s, k_\theta) - \sigma_n^2}{S_{g_i}(\omega_s, k_\theta) + (\beta - 1)\sigma_n^2} \tag{4}$$

where S_{gi} is the 2D discrete Fourier transform (FT) of sinogram $\boldsymbol{g_i}$ for image slice i and (ω_s, k_θ) denote the 2D FT coordinates. Notation β is a smoothing parameter, controlling the degree of smoothness and usually equal to 1 for SPECT study. In summary, the Anscombe transform, the K-L transform, and the Wiener filter lay down the framework of our approach to treatment of Poisson noise, as shown in Figure 2.

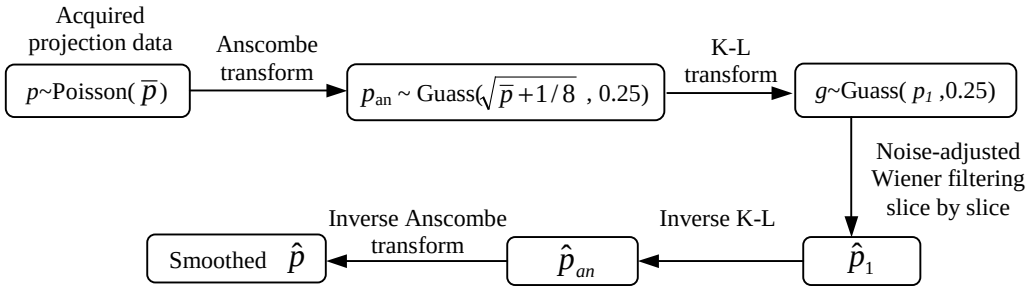

Figure 2. Diagram of proposed K-L domain noise-adjusted filtering.

2.2 Scatter Correction Based on a Triple-Energy-Window Acquisition Strategy

After suppression of Poisson noise, the scatter contribution to the primary-energy-window measurements is then removed by our scatter estimation method [24], which is based on the detection energy spectrum and modified from the triple-energy-window acquisition protocol [26]. In our triple energy window strategy, we selected one main window (W_m: 128 keV – 152 keV) centered at the peak energy of 140 keV, and two satellite windows (W_l and W_u with 4 keV width) centered at 126 keV and 154 keV respectively. The scattered photon counts within the main window is described as the following equation:

$$C_{sca} = \frac{2}{3} * \left(\frac{C_l}{W_l} - x.\frac{C_u}{W_u}\right) * W_m \tag{5}$$

where x is the ratio between C_l/W_l and C_u/W_u in the absence of attenuation and scatter, which removes the assumption that the primary photons inside both the satellite windows are the same [25, 26]. The value of x is determined by measuring a point source in air. When x value is equal to 1, our approach is close to the Bourguignon' method [25]. The scatter energy spectrum inside the photo-peak or main window (126-154 keV for Tc-99m tracer) is closely represented by a parabolic function rather than a linear function as assumed in both the Ogawa's and Bourguignon's methods [25, 26]. The area under the parabola spectrum can be accurately computed through an integral operation, given the heights at 126 keV and 154

keV locations. Therefore, a scale factor 2/3 rather than 1/2 is shown in our new algorithm. This non-linear scatter energy spectrum within the main window is fundamentally different from both the Ogawa's and Bourguignon's methods, in addition to the different treatment of primary photon counts in both the satellite windows.

2.3 Analytical Correction of Depth-Dependent Resolution Variation

For correction of DDRV, the inversion methods proposed up to date can provide either approximate solutions that realistically characterize the resolution kernel in a real SPECT system, or exact solutions that approximate the resolution kernel to some special functional forms in order to satisfy the mathematical derivations. Our previous study showed that an accurate consideration of the measured resolution kernel is needed to demonstrate robust performance and artifact-free reconstruction and, therefore, is a better choice for quantitative SPECT imaging [9]. In this study, the resolution variation is corrected by the depth-dependent deconvolution [18], which, being based on the central-ray approximation [2] and the distance-frequency relation [8], deconvolves the scatter-corrected data with the accurate detector-response kernel in frequency domain.

The depth-dependent deconvolution was detailed by Lewitt, *et al* [8] and Xia, *et al* [17] for reconstructing 2D images from 1D projections. Let $P(l,\omega_t)$ and $\tilde{P}(l,\omega_t)$ be the 2D Fourier transform (FT) of the sinogram $\{p_i\}$ and deblurred sinogram $\{\tilde{p}_i\}$, respectively, where l is the angular frequency and ω_t the spatial frequency, the distance-frequency relation is expressed as

$$P(l,\omega_t) = H(-l/\omega_t,\omega_t)\tilde{P}(l,\omega_t) \tag{6}$$

where $H(d,\omega_t)$ is the 1D FT of the 2D detector-response kernel h at depth d. The deconvolution is performed in frequency domain by

$$\tilde{P}(l,\omega_t) = H^{-1}(-l/\omega_t,\omega_t)P(l,\omega_t) \tag{7}$$

In practice, the inversion may not be usable, since $H(d, \omega_t)$ may include zeros or very small values. A modification is necessary [18]

$$H^{-1}(d,\omega_t) = H(d,\omega_t)/[H^2(d,\omega_t)+\varepsilon]$$

where ε is a small positive constant.

For 3D image reconstruction from 2D projections, the depth-dependent deconvolution of Eq.(7) is extended to

$$\tilde{P}(l,\omega_t,\omega_z) = H^{-1}(-l/\omega_t,\omega_t,\omega_z)P(l,\omega_t,\omega_z) \tag{8}$$

where ω_z is the spatial frequency in the z-axis, $\tilde{P}(l,\omega_t,\omega_z)$ and $P(l,\omega_t,\omega_z)$ are now the 3D FT of the 2D projection sinogram $\{\tilde{p}_i\}$ and $\{p_i\}$, respectively, and $H(d, \omega_t, \omega_z)$ becomes the 2D FT of the 3D detector response kernel $\{H^d_{i,j}\}$ at depth d. In this study, we correct the DDRV by 3D depth-dependent deconvolution based on Eq.(8).

2.4 Non-Uniform Attenuation Compensation Based on Novikov's Explicit Inversion Formula

After analytical compensation for the depth-dependent detector response, the deblurred projection data are finally represented by the attenuated Radon transform and can be reconstructed by the algorithm based on Novikov's explicit inversion formula with realistic human thoracic attenuation map.

Though uniform assumption may be applied in some situation like brain SPECT or abdomen SPECT where the object is mainly consisted of soft tissue, the attenuation coefficients across the human torso can't be considered as a constant. For uniform attenuation, Tretiak and Metz have developed an explicit inversion formula for uniform attenuated Radon transform or exponential Radon transform with parallel geometry [29]. Their algorithm assumes that the attenuation coefficient remains constant inside the body and the body contour is convex shaped. Some alternative inversion algorithms were developed later. Weng, *et al* extended the parallel-beam algorithm to fan-beam collimator geometry by a coordinate transform[30]. You, *et al.* derived a Cormack-type inversion of the exponential Radon transform by employing the circular harmonic transform directly in the projection space and the image space, instead of the Fourier space [31]. However, all these algorithms are for the uniform attenuation. They are not applicable for the regions with severe non-uniform attenuation, such as quantitative reconstruction of cardiac SPECT.

Novikov [34] and Natterer [20] have derived independently almost the same explicit inversion formula for non-uniform attenuated Radon transform recently. Kunyansky has implemented an SPECT reconstruction algorithm for parallel-hole collimators based on their inverse formula [19]. The numerical experiments showed that the use of the explicit inversion scheme allows for accurate image reconstruction even within the regions with severe non-uniform attenuation. In this study, we develop a similar reconstruction algorithm as Kunyansky did, and therefore the same notations will be used throughout this paper.

Let *f(x)* denote the object function to be reconstructed, *a(x)* be the attenuation coefficient map of the body tissues, and $g_\varphi(p)$ represent the projection datum at position *p* with projection angle φ. In order to simplify the expression of formula, a rotated coordinate system *(s, p)* is introduced:

$$s = x\cos\varphi + y\sin\varphi$$
$$p = -x\sin\varphi + y\sin\varphi$$

Then we have

$$g_\varphi(p) = \int_{-\infty}^{\infty} \exp(-D_\varphi a_\varphi(s,p)) f_\varphi(s,p)ds \tag{9}$$

where the divergent beam transform $D_\varphi a_\varphi(s, p)$ is defined as

$$D_\varphi a_\varphi(s,p) = \int_s^\infty a_\varphi(s,p)ds\,.$$

From explicit inverse formula for attenuated Radon transform, image *f(x)* can be reconstructed by:

$$f(x) = \frac{1}{4\pi}\int_0^{2\pi} \frac{\partial}{\partial p}(e^{(Da)(s,p)} ga(p))d\varphi\,, \tag{10}$$

where

$$ga(p) = e^{-A(p)}[\cos(HA(p))H\left(\cos(HA(p))e^{A(p)}g(p)\right) + \sin(HA(p))H\left(\sin(HA(p))e^{A(p)}g(p)\right)],$$
$$A(p) = \frac{1}{2}Ra(p)\,. \tag{11}$$

Among the two equations above, *R* stands for the Radon transform, *H* means the Hilbert transform, and *Da(s,p)* is the divergent beam transform of *a(p)*.

According to Eqs. (10) and (11), the reconstruction algorithm for non-uniform attenuation correction can be summarized as follows [19, 20, 34]:

- Computing the divergent beam transform $D_\varphi a_\varphi(s, p)$ and the Radon transform $Ra(p)$.
- Computing the modified projections $ga(p)$.
- Differentiating the result of $e^{(Da)(s,p)} ga(p)$ in p.
- Performing back-projection.

3. RESULTS

To evaluate the performance of our analytical reconstruction scheme, both numerical and Monte Carlo simulations (SIMIND, Ljungberg, *et al*. 1994) were used to generate realistic projection data from the MCAT digital torso phantom with defects inside myocardium. The attenuation map defined by MCAT was employed to generate attenuated projection data. The phantom was "scanned" by a SPECT system with high-resolution parallel-beam collimators and triple-energy-window acquisitions. The realistic detector-response kernel was also generated by Monte Carlo simulation on a high-density point source at 128 different depths from the collimator surface. The projection data were sampled on a grid of 128×128 per view over 128 views evenly spanning over 360°. If otherwise mentioned, the total counts for each view is approximately 2 millions and all the emission data were acquired by the same collimator geometric setting.

The performance of K-L domain adaptive Wiener filter is demonstrated in Figure 3. The total counts per view here is 200K. It reveals that the proposed adaptive Wiener filter does a better job in terms of filtering the Poisson noise in the degraded image over conventional spatial-invariant filtering, such Shepp-Logan filter and Hanning filter.

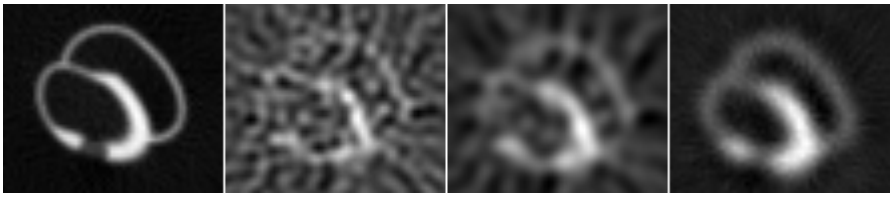

Figure 3: Comparison of transverse MCAT slices reconstructed using different filtering approaches. From left to right: noise-free, noisy data filtered by Shepp-Logan, Hanning, and K-L domain adaptive Wiener filter.

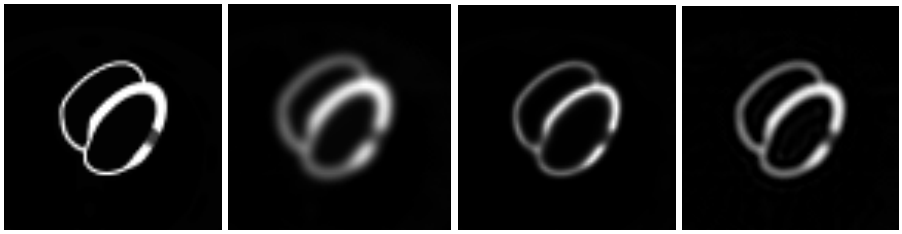

Figure 4: Reconstructed images from the simulated noise-free projections with iterative and analytical PSF correction. From left to right: activity phantom, PSF blurred image, maximum likelihood-expectation maximization with ordered subset (MLEM-OS) reconstruction, analytical reconstruction by our depth-dependent deconvolution.

Figure 4 shows the reconstructed image using different PSF correction. The 3D resolution kernel (or PSF function) representing the realistic detector response was generated by Monte Carlo simulation. The results demonstrate that the analytical method using depth-dependent deconvolution recovers resolution almost the same as that of iterative PSF correction. No obvious reconstruction artifact is observed in the analytically PSF corrected image. This further confirms our previous results that accurate consideration of the measured resolution kernel demonstrate robust performance and artifact-free reconstruction and, therefore, is a better choice for quantitative SPECT imaging.

Reconstruction in the case of severe non-uniform attenuation from the numerical simulations is shown in Figure 5. The phantom used here is the Shepp-Logan phantom. The artifacts caused by non-uniform attenuation can be clearly observed in the reconstructed image without attenuation correction, i.e. using the conventional filtered backprojection (FBP). Comparing the images in Figure 5, a significant improvement in image quality with the analytical reconstruction algorithm is seen, showing a correct implementation of our algorithm.

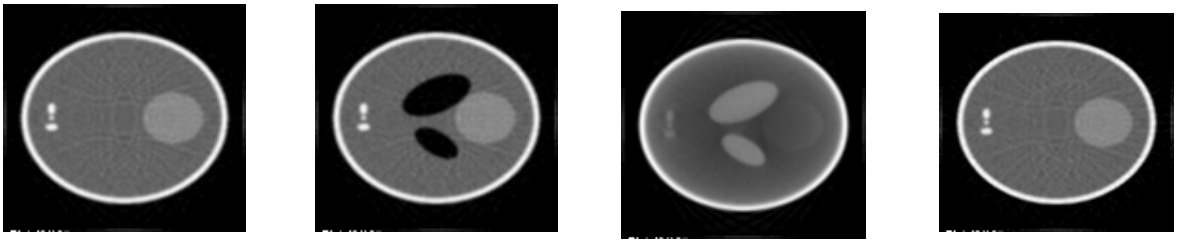

Figure 5: Reconstructions from noise-free numerically simulated projections. From left to right: activity phantom, attenuation Map, reconstruction without attenuation compensation (FBP), and reconstruction with attenuation compensation.

Reconstructed images from Monte Carlo simulations with different degradation factor correction are shown in Figure 6. The preliminary simulation results showed that the absolute value of the radiotracer-uptake ratios was greatly improved with the non-uniform attenuation, while the depth-dependent deconvolution significantly improved the image resolution as well as the absolute image value, as compared to the conventional FBP method. The proposed analytical reconstruction scheme is computationally comparable to FBP and quantitatively equivalent to iterative MAP-EM (maximum *a posteriori* expectation maximization) reconstruction with membrane prior.

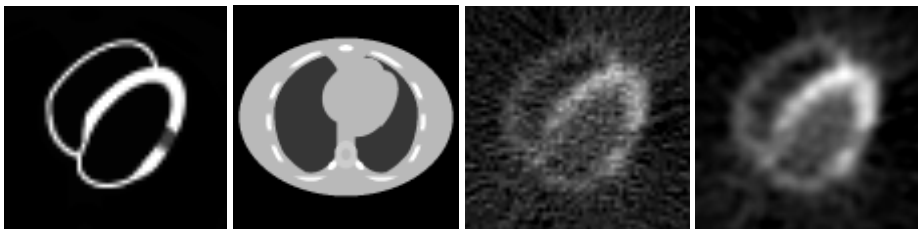

(a) (b) (c) (d)

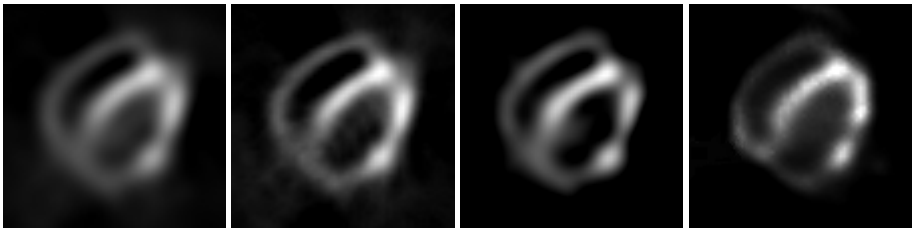

(e) (f) (g) (h)

Figure 6: MCAT phantom and reconstructed images from Monte Carlo simulations: (a) activity phantom, (b) attenuation map, (c) FBP reconstruction directly from noisy projections, (d) FBP with Hanning filter (fc=0.4), (e) FBP reconstruction with noise smoothing and scatter compensation, (f) FBP reconstruction with PSF, scatter correction, (g) proposed analytical scheme with attenuation, PSF, scatter correction, (h) MAP-EM-OS reconstruction after 20 iterations (Gaussian blur model).

4. CONCLUSION

In this paper, we described an analytical reconstruction scheme that provides a simultaneous compensation for non-uniform attenuation, object-specific scatter, and distance-dependent resolution variation, as well as accurate treatment of Poisson noise. From the numerical and Monte Carlo simulations, it is concluded that (i) the non-uniform attenuation compensation is necessary for accurate quantification, (ii) the correction of depth-dependent detector response improves the quantification significantly, especially performed before the attenuation correction, and (iii) accurate treatment of noise and scatter can greatly improve the utility of non-iterative methods for image reconstruction in 3D SPECT without significantly compromising the image resolution. Our preliminary results show clearly that analytical inversion for quantitative SPECT with simultaneous compensation for object-specific attenuation/scatter and distance-dependent collimator response, as well as accurate treatment of Poisson noise is feasible. This paper presents the work for parallel-hole collimators. Extension to other geometries is under progress[35].

ACKNOWLEDGEMENTS

This work was supported in part by the NIH National Heart, Lung and Blood Institute under Grant No. HL54166.

REFERENCES

1. BMW Tsui, GT Gullberg, ER Edgerton, and *et al*, "Correction of nonuniform attenuation in cardiac SPECT imaging", *J. Nucl. Med.* **30**, pp. 497-507, 1991
2. Z Liang, TG Turkington, DR Gilland, and *et al*, "Simultaneous compensation for attenuation, scatter, and detector response for SPECT reconstruction in three dimensions", *Phys. Med. Biol.* **37**, pp. 587-603, 1992
3. JW Wallis and TR Miller, "Rapidly converging iterative reconstruction algorithms in SPECT", *J. Nucl. Med.* **34**, pp. 1793-800, 1993
4. XL Xu, JS Liow, and SC Strother, "Iterative algebraic reconstruction algorithms for ECT: A unified framework and its application to PET", *Med. Phys*. **20**, pp. 1675-84, 1993
5. GL Zeng, GT Gullberg, BMW Tsui, and *et al*, "Three dimensional iterative reconstruction algorithms with attenuation and geometric point response correction", *IEEE Trans. Nucl. Sci*. **NS-38**, pp. 693-702, 1991
6. SJ Glick, BC Penny, MA King, and CL Byrne, "Noniterative compensation for the distance-dependent detector response and photon attenuation in SPECT imaging", *IEEE Trans. Med. Imag.* **13**, pp. 363-374, 1994

7. SJ Glick, WG Hawkins, MA King, and *et al*, "The effect of intrinsic attenuation correction methods on the stationarity of the 3-D modulation transfer function of SPECT", *Med. Phys.* **19**, pp. 1105-1112, 1992
8. RM Lewitt, PR Edholm, and W Xia, "Fourier method for correction of depth-dependent collimator blurring", *Proc. SPIE*, **1092**, pp. 232-243, 1989
9. J Li, Z Liang, J Ye, and G Han, "Implementation and preliminary investigation of analytical methods for correction of distance-dependent resolution variation and uniform attenuation in 3D brain SPECT", *IEEE Trans. Nucl. Sci.* **46**, pp. 2162-2171, 1999
10. Z Liang, J Ye, J Cheng, and DP Harrington, "Quantitative brain SPECT in three dimensions: an analytical approach to non-uniform attenuation without transmission scans", in *Computational Imaging and Vision* book series, by Kluwer Academic Publishers, pp.117-132, 1996.
11. CE Metz and X Pan, "A unified analysis of exact methods of inverting the 2-D exponential Radon transform, with implications for noise control in SPECT", *IEEE Trans. Med. Imag.* **14**, pp. 643-658, 1995
12. X Pan and CE Metz, "Non-iterative methods and their noise characteristics in 2D SPECT image reconstruction", *IEEE Trans. Nucl. Sci.* **44**, pp. 1388-1397, 1997
13. X Pan, CE Metz, and CT Chen, "A class of analytical methods that compensate for attenuation and spatially-variant resolution in 2D SPECT", *IEEE Trans. Nucl. Sci.* **43**, pp. 2244-2254, 1996
14. EJ Soares, SJ Glick, and MA King, "Noise Characterization of combined Bellini-type attenuation correction and frequency-distance principle restoration filtering", *IEEE Trans. Nucl. Sci.* **43**, pp. 3278-3290, 1996
15. BMW Tsui, EC Frey, X Zhao, and *et al*, "The importance and implementation of accurate 3D compensation methods for quantitative SPECT", *Phys. Med. Biol.* **39**, pp. 509-530, 1994
16. L van Elmbt and S Walrand, "Simultaneous correction of attenuation and distance-dependent resolution in SPECT: an analytical approach", *Phys. Med. Biol.* **38**, pp. 1207-1217, 1993
17. W Xia, RM Lewitt, and PR Edholm, "Fourier correction for spatially variant collimator blurring in SPECT", *IEEE Trans. Med. Imag.* **14**, pp. 100-115, 1995
18. J Ye, Z Liang, and DP Harrington, "Quantitative reconstruction for myocardial perfusion SPECT: an efficient approach by depth-dependent deconvolution and matrix rotation", *Phys. Med. Biol*. **39**, pp. 1263-1279, 1994
19. L Kunyansky, "A new SPECT reconstruction algorithm based on the Novikov's explicit inversion formula", *Inverse Problems*, **17**, pp. 293-306, 2001
20. F Natterer, "Inversion of the attenuated Radon transform", *Inverse Problems*, **17**, pp. 113-119,2001
21. FJ Anscombe, "The transformation of Poisson, binomial and negative-binomial data", *Biometrics*, **35**, pp. 246-254, 1948
22. H Lu, D Chen, L Li, and *et al*, "A combined transformation of ordering SPECT sinograms for signal extraction from measurements of Poisson noise", *SPIE Medical Imaging*, **4322**, pp. 943-951, 2001.
23. BR Hunt and O Kübler, "Karhunen-Loeve multi-spectral image restoration, part I: theory", *IEEE Trans. Acoustics, Speech, and Signal Processing*, **ASSP-32**, pp. 592-600, 1984
24. X Li, G. Han, H Lu, L Li, and Z Liang, "A new scatter estimation method using triple window acquisition to fit energy spectrum", *J. Nucl. Med.* **42**, pp. 194, 2001
25. MH Bourguignon, M Wartski, N Amokrane, *et al*, "Le spectre du rayonnement diffusé dans la fenêtre du photopic: analyse et proposition d'une methode de correction", *Médecine Nucléaire*, **17**, pp. 53-58, 1993
26. K Ogawa, Y Harata, T Ichihara, A Kubo, and S Hashimoto, "A practical method for position dependent Compton scatter correction in SPECT," *IEEE Trans. Med. Imag.* **10**, pp. 408-412, 1991
27. BC Penney, SJ Glick, and MA King, "Relative importance of the error sources in Wiener restoration of scintigrams," *IEEE Trans. Med. Imag.* **9**, pp. 60-70, 1990
28. B Xu, X Pan, and CT Chen, "An innovative method to compensate for distance-dependent blurring in 2D SPECT", *IEEE Trans. Nucl. Sci.* **45**, pp. 2245-2252, 1998
29. OJ Tretiak and CE Metz, "The exponential radon transform SIAM", *J. Appl. Math.* **39**, pp. 341-54, 1980
30. Y. Weng, L. Zeng, and GT Gullberg, "Analytical inversion formula for uniformly attenuated fan-beam projections", *IEEE Tans. Nucl. Sci.* **44**, pp. 243-249, 1997
31. J You, Z Liang, and G Zeng, "A unified reconstruction framework for both parallel-beam and variable focal-length fan-beam collimators by a Cormack-type inversion of exponential Radon transform", *IEEE Trans. Med. Imag.* **18**, pp. 59-65, 1999
32. CM Kao and X Pan, "Non-iterative methods incorporating *a prior* source distribution and data information for suppression of image noise and artifacts in 3D SPECT", *Phys. Med. Biol.* **45**, pp. 2801-2819, 2000
33. CM Kao and X Pan, "Toward optimal non-iterative reconstruction for 3D SPECT with uniform attenuation and distance-dependent spatial resolution", *Conference Record of IEEE NSS and MIC* (CD-ROM), 2000

34. R Novikov, “An inversion formula for the attenuated X-ray transformation”, Preprint, May 2000
35. J. Wen, T Li, X Li, and et al, “Fan-beam and variable-focal-length fan-beam SPECT reconstruction with non-uniform attenuation”, 49th Annual Meeting of Society of Nuclear Medicine, 2002 (submitted)